島根大学地球資源環境学研究報告　32, 23～31 ページ（2013 年 12 月）
Geoscience Rept. Shimane Univ., 32, p.23～31（2013）

Article

Clinopyroxenes in garnet–aegirine-augite schists from the Sambagawa metamorphic belt, Bizan district, eastern Shikoku, Japan

Masaaki Kainuma*, Akira Takasu* and Md. Fazle Kabir*

Abstract

The Sambagawa metamorphic belt in the Bizan district consists mainly of pelitic schists, basic schists, and siliceous schists, along with minor garnet glaucophane schists. Siliceous schists containing garnet and clinopyroxene (garnet–aegirine-augite schists) are found within pelitic schists in both spotted and non-spotted schist zones. Garnet–aegirine-augite schists collected from the spotted schist zone consist mainly of quartz and phengite, with minor amounts of amphibole (ferroglaucophane, magnesioriebeckite, riebeckite, magnesiokatophorite, winchite, barroisite, ferrobarroisite), garnet, clinopyroxene (aegirine-augite, aegirine, omphacite; X_{Jd} 0.08-0.37) and albite. Hematite, ilmenite, chlorite, epidote, calcite and titanite occur occasionally. Clinopyroxenes are found in two modes of occurrence: firstly, as inclusions in albite porphyroblasts (Cpx1), and secondly within the matrix (Cpx2). Most of the clinopyroxenes are zoned, with jadeite component-rich cores and jadeite-poor rims. This zoning represents decreasing jadeite component due to the decrease in pressure that occurred after the peak metamorphism. The jadeite component of Cpx1 is greater than that of Cpx2, suggesting that the composition of the clinopyroxenes was preserved within the albite porphyroblasts.

Key words: Sambagawa (Sanbagawa), Bizan area, clinopyroxene, aegirine-augite, omphacite.

Introduction

The Sambagawa metamorphic belt is classified as an intermediate high-pressure type metamorphic belt by Miyashiro (1973), and formed in a subduction zone setting (Takasu *et al.*, 1994; Wallis, 1998). It mainly consists of metasedimentary and metavolcanic rocks that originated in oceanic environments, and subsequently underwent metamorphism related to Cretaceous subduction. To the north the Sambagawa belt is bounded by the Ryoke belt, which is characterized by low *P/T* metamorphism. These together form the best-known example of paired metamorphic belts (Miyashiro, 1961). The boundary between the Sambagawa and Ryoke belts is a major strike-slip fault, the Median Tectonic Line (MTL). The protoliths of the Sambagawa metamorphic belt are dominantly sandstones and shales, with a small amount of basaltic volcaniclastic rocks, cherts, and limestones. Petrologic studies show that the metamorphic conditions of the Sambagawa belt correspond to the pumpellyite-actinolite, greenschist, blueschist and epidote-amphibolite facies (Banno and Sakai, 1989; Otsuki and Banno, 1990; Enami *et al.*, 1994).

In the Besshi district in central Shikoku, the metamorphism is divided into chlorite, garnet, albite-biotite and oligoclase-biotite zones in order of increasing metamorphic grade, based on the mineral parageneses of pelitic schists (Enami, 1983; Higashino, 1990). The higher-grade albite-biotite and oligoclase-biotite zones are extensively distributed in the Besshi district. The metamorphic grade of these mineral zones is equivalent to that of the epidote-amphibolite facies, and *P-T* conditions have been estimated to be 7-10 kbar and 480-620°C (Enami *et al.*, 1994; Wallis *et al.*, 2000). Eclogite facies assemblages sporadically occur in metagabbros, metabasites, peridotites, and minor amounts of metapelites in the Besshi district in central Shikoku (e.g. Banno *et al.*, 1976; Takasu, 1984; Kunugiza *et al.*, 1986; Takasu, 1989; Aoya, 2001; Ota *et al.*, 2004; Zaw Win Ko *et al.*, 2005; Kabir and Takasu, 2010a, b). Eclogites occur in the Besshi district, mainly within block-like bodies of varying size and lithology (Kunugiza *et al.*, 1986; Takasu, 1989; Takasu *et al.*, 1994).

The Kotsu-Bizan area is located in eastern Shikoku (Fig. 1). The Kotsu and Bizan areas are located in the same tectonostratigraphic horizon, i.e. the Kotsu Formation in eastern Shikoku. The Kotsu Formation is structurally overlain and underlain by the Kawata and Kawatayama Formations, respectively (Fig. 1). The main rock types in the Bizan area include pelitic, basic, and siliceous schists, with minor amounts of psammitic and calcareous schists (Iwasaki, 1963). Basic and pelitic schists show large-scale alternation, and siliceous schists occur as lenses or thin layers within these alterations. Faure (1983) suggested that the Bizan area is a mélange zone containing tectonic blocks of serpentinite, metagabbro and garnet-amphibolite (garnet-glaucophane schist) occurring along a ductile shear zone between spotted and non-spotted schist zones.

Iwasaki (1963) reported the occurrence of magnesioriebeckite bearing garnet–aegirine-augite–alkali amphibole–quartz schists (garnet–aegirine-jadeite–alkali amphibole–quartz schist) from the Bizan area. Enami *et al.* (1994) also reported the occurrence of sodium pyroxene in quartz schist from the Sambagawa metamorphic belt in the central Shikoku.

In this paper we describe garnet and clinopyroxene-bearing

*Department of Geoscience, Graduate School of Science and Engineering, Shimane University, 1060 Nishikawatsu, Matsue 690-8504, Japan

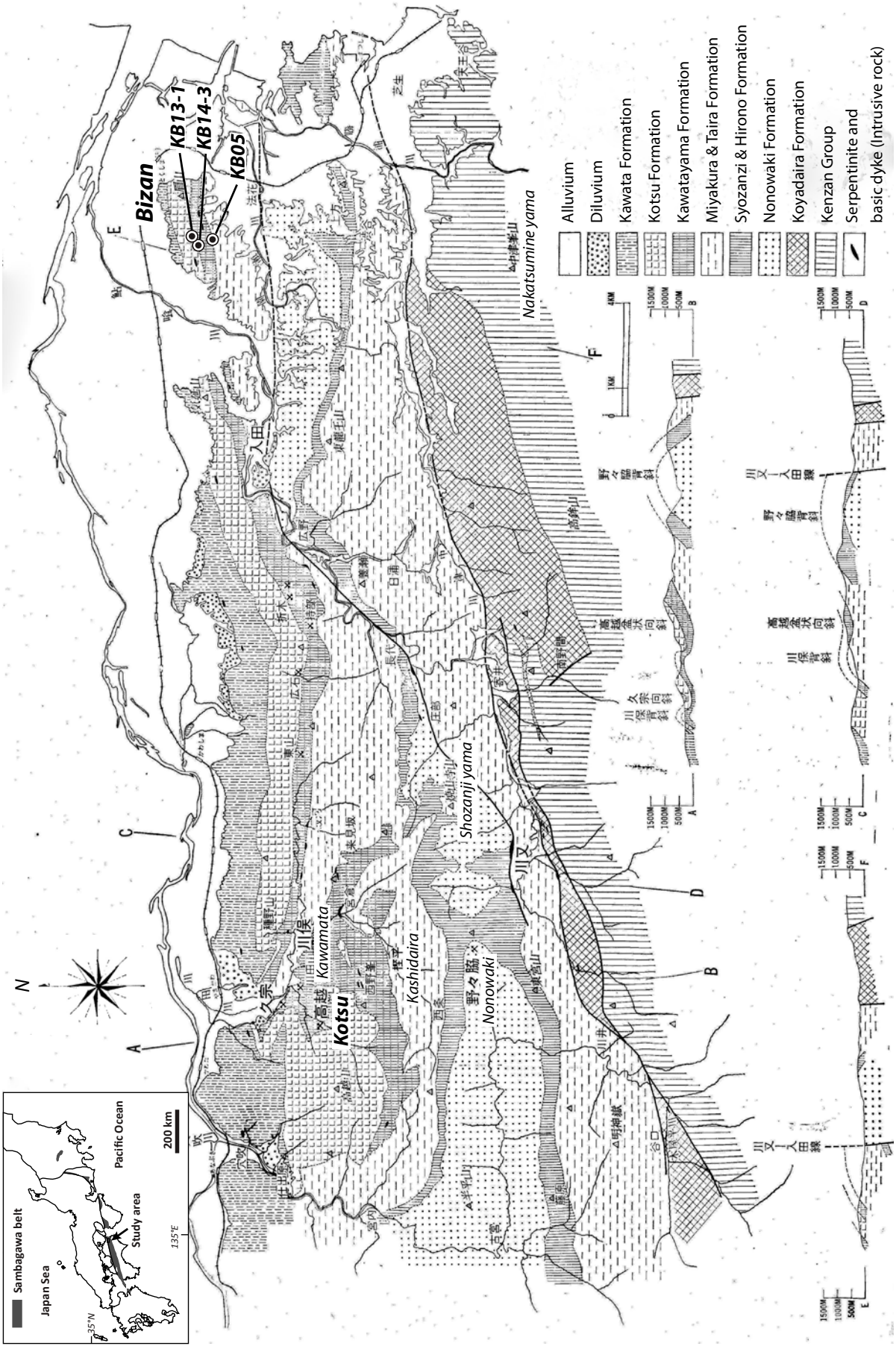

Fig. 1. Geological map of the Sambagawa metamorphic belt in the Kotsu-Bizan area, eastern Shikoku, Japan (after Kenzan Research Group, 1963), and sample localities.

siliceous schists intercalated within pelitic schists in both the spotted and non-spotted schist zones in the Bizan area. Samples were collected from the Fukumandani Valley. Two samples (KB13-1 and KB14-3) were collected from the spotted schist zone, and one sample (KB05) from the non-spotted schist zone. The garnet–aegirine-augite schists have been described by Kainuma *et al.* (2012). Clinopyroxenes occur in two modes of occurrence, firstly as inclusions in porphyroblastic albite (Cpx1) and secondly in the matrix (Cpx2) (Figs. 2 and 3). Here we report the mineral chemistry and zoning of clinopyroxenes within the garnet–aegirine-augite schists.

The mineral abbreviations used in the text, tables and figures follow Whitney and Evans (2010) except for Aeg-Aug, aegirine-augite.

Chemical compositions of the amphiboles

Chemical compositions and zoning of clinopyroxenes in the garnet–aegirine-augite schists from the Bizan area were examined at Shimane University using two electron probe micro analyzers (JEOL JXA-8800M and JXA-8530F). Analytical conditions used were 15 kV accelerating voltage, 20 nA specimen current and 5 μm beam diameter. Correction procedures were carried out as described by Bence and Albee (1968). The classification of the clinopyroxenes was made using the method of Morimoto (1989). Fe^{3+} estimation for clinopyroxene used $Fe^{3+} = 4 - 2 \times Si - 2 \times Ti - Al + Na$ (for 6 oxygens). The chemical compositions of clinopyroxenes in all modes of occurrence are listed in Table 1.

KB13-1:

Clinopyroxenes occur as two modes, as inclusions in porphyroblastic albite (Cpx1) and in the matrix (Cpx2) (Fig. 2a-c). Clinopyroxenes (Cpx1) occurring as inclusions in porphyroblastic albite are mostly classified as aegirine-augite, minor aegirine, and omphacite, with X_{Jd} 0.10-0.37, X_{Aeg} 0.34-0.62 and X_{Aug} 0.12-0.46 compositions (Fig. 4a). Some are compositionally zoned, with decreasing X_{Jd} (0.34-0.21) and increasing X_{Aug} (0.26-0.40) from cores to rims (Figs. 4a and 5a).

Clinopyroxenes occurring in the matrix (Cpx2) are classified as aegirine-augite with lower X_{Jd} (X_{Jd} 0.16-0.25, X_{Aeg} 0.34-0.57, X_{Aug} 0.23-0.48) than those occurring as inclusions in porphyroblastic albites (Fig. 4a). Some clinopyroxenes are compositionally zoned, with decreasing X_{Jd} (0.22-0.17), and X_{Aeg} (0.36-0.40) increasing, and then slightly decreasing X_{Aug} (0.41-0.48-0.42) from cores to rims (Figs. 4a and 5b).

KB14-3:

The clinopyroxenes in this sample also have two modes of occurrence. Clinopyroxenes (Cpx1) occurring as inclusions in porphyroblastic albite are mostly classified as aegirine-augite and minor aegirine, with X_{Jd} 0.08-0.35, X_{Aeg} 0.37-0.72 and X_{Aug} 0.15-0.45 (Figs. 2d-f and 4b). Aegirine-augite (Cpx1) displays slight zoning with decreasing X_{Jd} (0.29-0.20) and X_{Aeg} (0.41-0.39) and increasing X_{Aug} (0.29-0.40) from core to the rim (Figs. 4b and 5c).

Clinopyroxenes in the matrix (Cpx2) are aegirine-augite and aegirine, with lower X_{Jd} (X_{Jd} 0.10-0.27, X_{Aeg} 0.38-0.65, X_{Aug} 0.17-0.45) than Cpx1 (Fig. 4b). Matrix clinopyroxenes (Cpx2) are sometimes zoned, with decreasing X_{Jd} (0.25-0.12), increasing X_{Aeg} (0.42-0.54), and increasing and then slightly decreasing X_{Aug} (0.33-0.42-0.32) to the rims (Figs. 4b and 5d).

KB05:

Clinopyroxene occurs only in the matrix in this sample. The clinopyroxene is aegirine-augite with composition of X_{Jd} (0.09-0.21), X_{Aeg} (0.36-0.51) and X_{Aug} (0.37-0.51) (Figs. 3a-b and 4c). Most of the clinopyroxenes are zoned, with cores having lower jadeite contents (X_{Jd} 0.13), increasing in the mantle (X_{Jd} 0.19) and then decreasing further at the rims (X_{Jd} 0.12) (Figs. 4c and 5e).

Discussion and Conclusions

Clinopyroxenes in the garnet–aegirine-augite schists from the Fukumandani Valley in the Bizan area exhibit two modes of occurrence, and a wide range of chemical compositions with distinct zoning patterns. Clinopyroxenes occurring in samples KB13-1 and KB14-3 are aegirine-augite, aegirine and omphacite (X_{Jd} 0.08-0.37), whereas those in sample KB05 are aegirine-augite (X_{Jd} 0.09-0.21). The jadeite content of matrix clinopyroxenes is lower (X_{Jd} 0.09-0.27) than the clinopyroxene inclusions in porphyroblastic albite (X_{Jd} 0.08-0.37). This probably suggests that jadeite-rich clinopyroxene compositions are preserved within the albite porphyroblasts.

Most clinopyroxenes in KB13-1 and KB14-3 (both as inclusions in porphyroblastic albite and in the matrix) are zoned, with jadeite-rich cores and jadeite-poor rims, suggesting retrograde zoning. Matrix clinopyroxenes may have been decomposed into albite during exhumation. Jadeite contents in clinopyroxenes decrease by the reaction of Jd + Qtz = Ab, during decreasing pressure through exhumation.

Some aegirine-augites in sample KB05 are zoned, with increasing and then decreasing X_{Jd} (0.13-0.19-0.12) from core to the rim. This zoning pattern indicates that most of the prograde-zoned clinopyroxenes were partially destroyed during the decompression metamorphism. Clinopyroxenes with much higher jadeite contents may thus have been present during the prograde and peak metamorphic stages.

Iwasaki (1963) reported the occurrence of clinopyroxene (X_{Jd} 0.30) in the garnet–aegirine-augite–alkali amphibole–quartz schists (garnet–aegirine-jadeite–alkali amphibole–quartz schist) from the Bizan area. Enami *et al.* (1994) reported the occurrence of sodic pyroxenes in quartz schists in the Sarutagawa (X_{Jd} 0.17-0.30), Asemigawa (X_{Jd} 0.15-0.19) and Besshi areas (X_{Jd} 0.11-0.19) of the Sambagawa metamorphic belt in central Shikoku (Fig. 4d). Enami *et al.* (1994) estimated metamorphic pressures using jadeite contents in clinopyroxene in the albite-biotite zone, giving values of 8-9.5 kbar in the

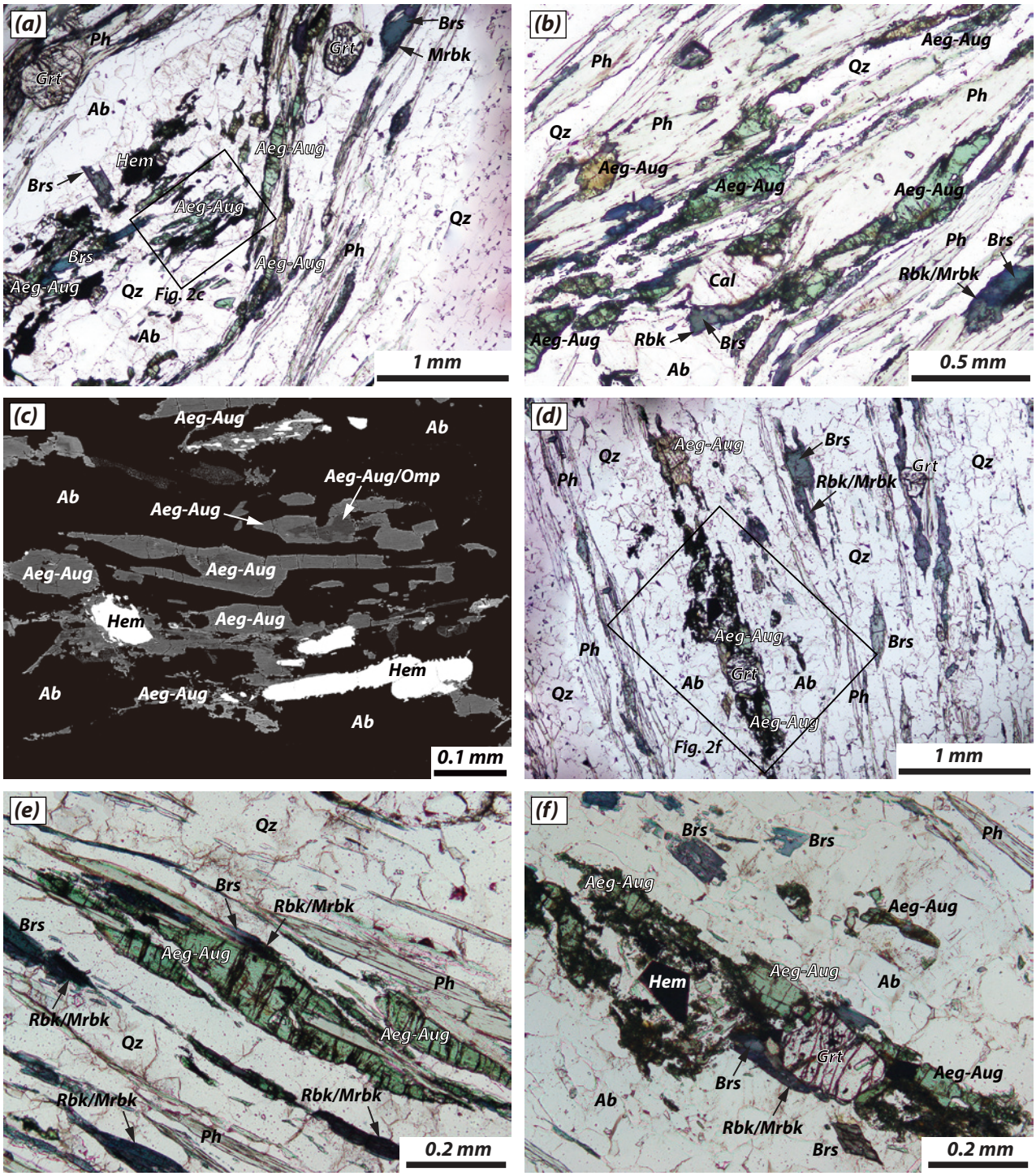

Fig. 2. Photomicrographs and a backscattered electron image (BEI) of garnet–aegirine-augite schists from the Bizan area showing textural relationships of clinopyroxene with other minerals. (a) Porphyroblastic albite, and matrix minerals including garnet, aegirine-augite, amphibole (barroisite core and magnesioriebeckite rim), phengite and quartz (KB13-1). Porphyroblastic albite contains inclusions of aegirine-augite, barroisite, hematite and quartz. (b) Photomicrograph showing schistosity-forming matrix clinopyroxenes in sample KB13-1. Most of the clinopyroxenes are zoned, with pleochroism of X'=colorless and Z'=pale green. Other matrix minerals are garnet, amphibole (barroisite cores and riebeckite/magnesioriebeckite rims), phengite, albite, calcite and quartz (KB13-1). (c) BEI of zoned clinopyroxene inclusions in porphyroblastic albite, with zoning from omphacite and aegirine-augite cores to aegirine-augite rims (KB13-1). (d) Porphyroblastic albite containing inclusions of aegirine-augite, garnet and hematite. Matrix minerals are garnet, aegirine-augite, phengite, amphibole (barroisite cores and riebeckite/magnesioriebeckite rims) and quartz (KB14-3). (e) Photomicrograph showing schistosity-forming matrix clinopyroxene, with other matrix minerals including amphibole (barroisite cores and riebeckite/magnesioriebeckite rims), phengite and quartz (KB14-3). (f) Photomicrograph showing clinopyroxene inclusions in porphyroblastic albite coexisting with garnet (KB14-3). Barroisitic amphibole and hematite also occur as inclusions.

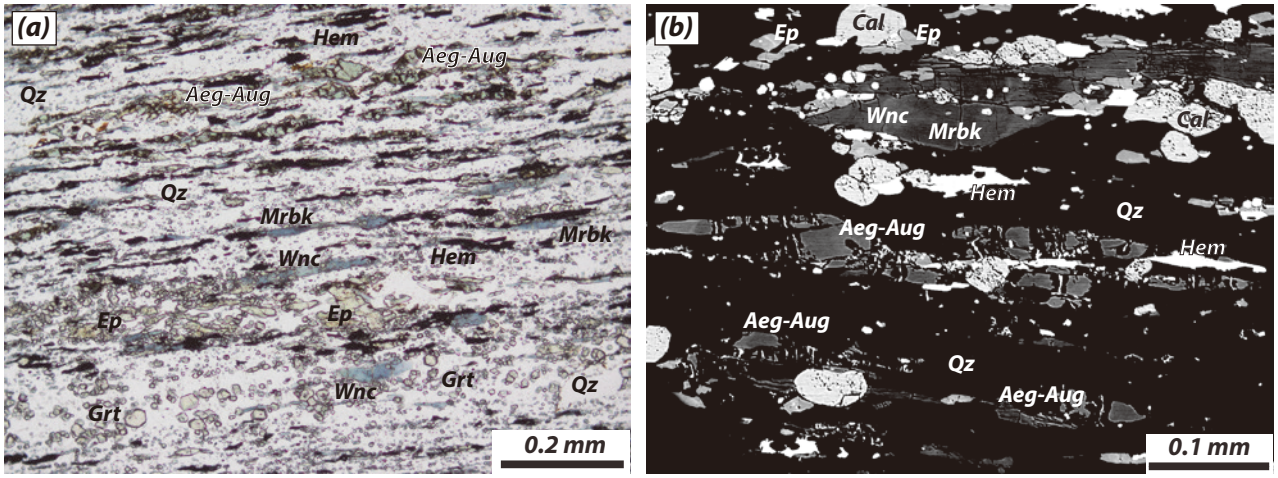

Fig. 3. Photomicrographs and a backscattered electron image of garnet–aegirine-augite schist (sample KB05) from the Bizan area. (a) Aegirine-augite and other schistosity-forming matrix minerals including garnet, epidote, amphibole (magnesioriebeckite and winchite), hematite and quartz. (b) Zoned aegirine-augite in the matrix, core is slightly darker than the rim. The other matrix minerals are epidote, amphibole (magnesioriebeckite and winchite), hematite, calcite and quartz.

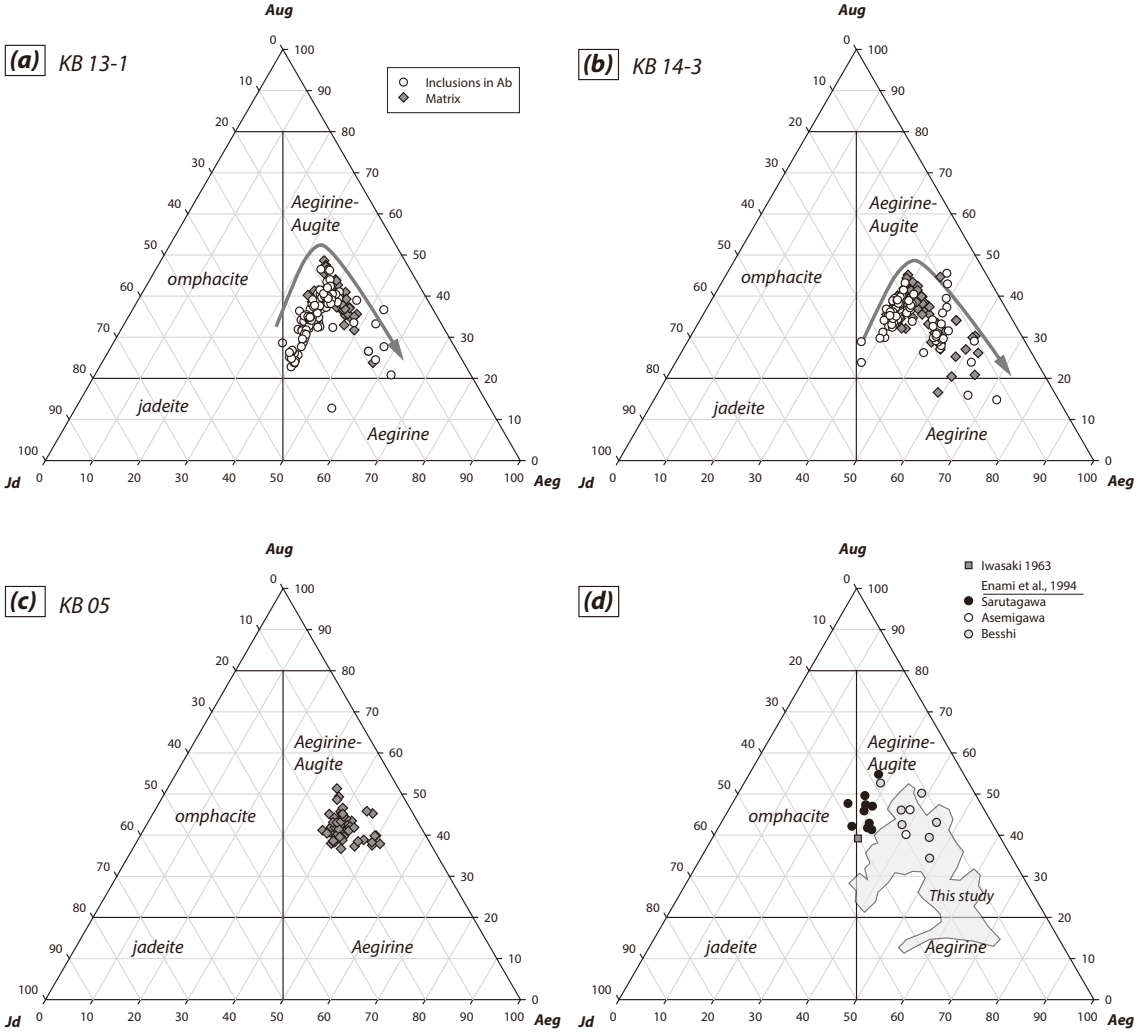

Fig. 4. Chemical compositions of clinopyroxenes from the garnet–aegirine-augite schists, (a) sample KB13-1, (b) KB-14-3 and (c) KB05. (d) Comparison of the distribution of data from this study with clinopyroxenes from garnet–aegirine-jadeite–alkali amphibole–quartz schists from the Bizan area (Iwasaki, 1963) and sodic pyroxene-bearing quartz schists from the Sarutagawa, Asemigawa and Besshi areas, Sambagawa metamorphic belt, central Shikoku (Enami *et al.*, 1994).

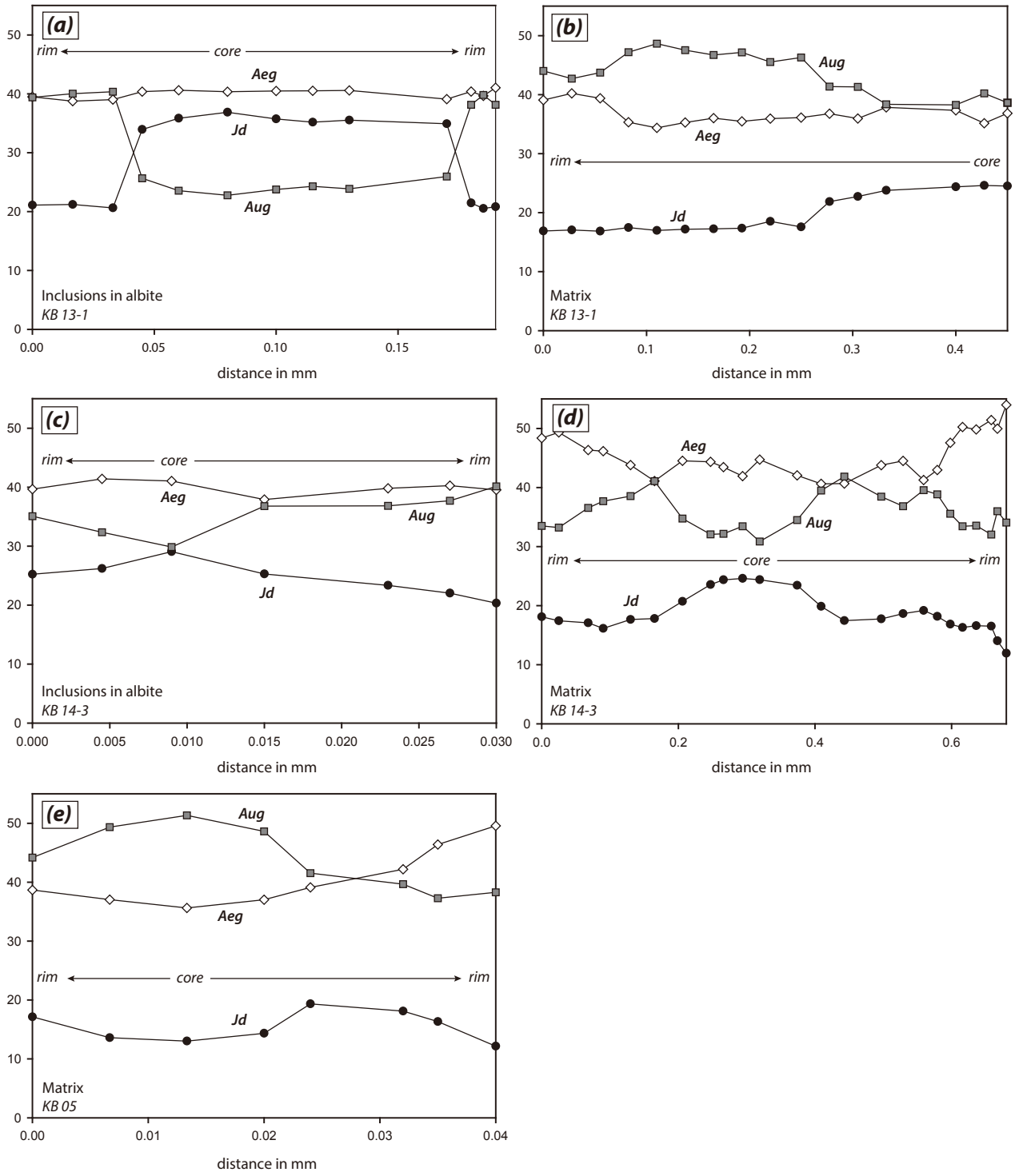

Fig. 5. Compositional zoning of clinopyroxenes from the garnet–aegirine-augite schists, (a-b) KB13-1, (c-d) KB-14-3 and (e) KB05.

Asemigawa and Besshi area and 10.5-11 kbar in Sarutagawa area. In contrast, jadeite contents of the clinopyroxenes in the garnet clinopyroxene schists examined here are significantly greater than those of the garnet–aegirine-augite–alkali amphibole–quartz schists (Iwasaki, 1963) and in the Asemigawa, Besshi and Sarutagawa areas (Enami *et al.*, 1994). This higher jadeite content in the clinopyroxenes in the Bizan garnet–aegirine-augite schists suggests that metamorphic pressures in this occurrence may have have been greater than those reported by Enami *et al.* (1994) for the Sambagawa metamorphism in central Shikoku. Further research is needed to estimate the metamorphic *P-T* conditions of the garnet–aegirine-augite schists within the pelitic schists in the Bizan area.

Acknowledgements

We thank B. P. Roser for his careful reading and constructive comments on the manuscript, and members of the Geoscience seminar and Metamorphic Geology seminar of Shimane University for discussion and helpful suggestions. This study was partly supported by JSPS KAKENHI Grant (No. 24340123) to A.T.

References

Aoya, M., 2001, *P-T-D* path of eclogite from the Sambagawa belt deduced from combination of petrological and microstructural analyses. *Journal of Petrology*, **42**, 1225-1248.

Banno, S. and Sakai, C., 1989, Geology and metamorphic evolution of the Sanbagawa metamorphic belt, Japan. In: *Evolution of Metamorphic Belts* (eds Daly, J. S., Cliff, R. A. & Yardley, B. W. D.), pp. 519-532, Blackwell Scientific Publications, Oxford, Geological Society, London.

Banno, S., Yokohama, K., Enami, M., Iwata, O., Nakamura, K. and Kasashima, S., 1976, Petrography of the peridotite-metagabbro complex in the vicinity of Mt. Higashi-akaishi, Central Shikoku. Part I. Megascopic textures of the Iratsu and Tonaru epidote amphibolite massas. *The Science Reports of Kanazawa University*, **21**, 139-159.

Bence, A. E. and Albee, A. L., 1968, Empirical correction factors for the electron microanalysis of silicates and oxides. *Journal of Geology*, **76**, 382-403.

Enami, M., 1983, Petrology of pelitic schists in the oligoclase-biotite zone of the Sanbagawa metamorphic terrain, Japan: phase equilibria in the highest grade zone of a high-pressure intermediate type of metamorphic belt. *Journal of Metamorphic Geology*, **1**, 141-161.

Enami, M., Wallis, S. R. and Banno, Y., 1994, Paragenesis of sodic pyroxene-bearing quartz schists: implications for the *P-T* history of the Sanbagawa belt. *Contributions to Mineralogy and Petrology*, **116**, 182-198.

Faure, M., 1983, Eastward ductile shear during the early tectonic phase in the Sanbagawa belt. *Journal of the Geological Society of Japan*, **89**, 319-329.

Higashino, T., 1990, The higher grade metamorphic zonation of the Sambagawa metamorphic belt in central Shikoku, Japan. *Journal of Metamorphic Geology*, **8**, 413-423.

Iwasaki, M., 1963, Metamorphic rocks of the Kotu-Bizan area, eastern Shikoku. *Journal of the Faculty of Science, University of Tokyo, Section II*, **15**, 1-90.

Kabir, M. F. and Takasu, A., 2010a, Evidence for multiple burial-partial exhumation cycles from the Onodani eclogites in the Sambagawa metamorphic belt, central Shikoku, Japan. *Journal of Metamorphic Geology*, **28**, 873-893.

Kabir, M. F. and Takasu, A., 2010b, Glaucophanic amphibole in the Seba eclogitic basic schists, Sambagawa metamorphic belt, central Shikoku, Japan: implications for timing of juxtaposition of the eclogite body with the non-eclogite Sambagawa schists. *Earth Sciences (Chikyu Kagaku)*, **64**, 183-192.

Kainuma, M., Takasu, A. and Kabir, M. F., 2012, Amphiboles in garnet–aegirine-augite schists from the Sambagawa metamorphic belt, Bizan district, eastern Shikoku, Japan. *Geoscience Reports of Shimane University, Japan*, **31**, 23-32.

Kenzan Research Group, 1963, Geology of the crystalline schist region of Eastern Shikoku. *Earth Science*, **69**, 16-19 (in Japanese with English abstract).

Kunugiza, K., Takasu, A. and Banno, S., 1986, The origin and metamorphic history of the ultramafic and metagabbro bodies in the Sanbagawa Metamorphic Belt. *Geological Society of America Memoir*, **164**, 375-386.

Miyashiro, A., 1961, Evolution of metamorphic belts. *Journal of Petrology*, **2**, 277-311.

Miyashiro, A., 1973, *Metamorphism and metamorphic belts*. George Allen and Unwin, London, England.

Morimoto, N., 1989, Nomenclature of pyroxenes. *The Canadian Mineralogist*, **27**, 143-156.

Ota, T., Terabayashi, M. and Katayama, I., 2004, Thermobaric structure and metamorphic evolution of the Iratsu eclogite body in the Sanbagawa belt, central Shikoku, Japan. *Lithos*, **73**, 95-126.

Otsuki, M. and Banno, S., 1990, Prograde and retrograde metamorphism of hematite-bearing basic schists in the Sambagawa belt in central Shikoku. *Journal of Metamorphic Geology*, **8**, 425-439.

Takasu, A., 1984, Prograde and retrograde eclogites in the Sambagawa metamorphic belt, Besshi district, Japan. *Journal of Petrology*, **25**, 619-643.

Takasu, A., 1989, *P-T* histories of peridotite and amphibolite tectonic blocks in the Sanbagawa metamorphic belt, Japan. In: *Evolution of Metamorphic Belts* (eds Daly, J. S., Cliff, R. A. & Yardley, B. W. D.), pp. 533-538, Blackwell Scientific Publications, Oxford, Geological Society, London, Special Publications.

Takasu, A., Wallis, S. R., Banno, S. and Dallmeyer, R. D., 1994, Evolution of the Sambagawa metamorphic belt, Japan. *Lithos*, **33**, 119-133.

Wallis, S. R., 1998, Exhuming the Sanbagawa metamorphic belt: the importance of tectonic discontinuities. *Journal of Metamorphic Geology*, **16**, 83-95.

Wallis, S., Takasu, A., Enami, M. and Tsujimori, T., 2000, Eclogite and related metamorphism in the Sanbagawa belt, Southwest Japan. *Bulletin of the Research Institute of Natural Sciences, Okayama University of Science*, **26**, 3-17.

Whitney, D. L. and Evans, B. W., 2010, Abbreviations for names of rock-forming minerals. *American Mineralogist*, **95**, 185-187.

Zaw Win Ko, Enami, M. and Aoya, M., 2005, Chloritoid and barroisite-bearing pelitic schists from the eclogite unit in the Besshi district, Sanbagawa metamorphic belt. *Lithos*, **81**, 79-100.

(Received: Nov. 22, 2013, Accepted: Dec. 6, 2013)

（要　旨）

貝沼雅亮・高須　晃・Kabir Md. Fazle，2013 四国東部眉山地域三波川変成帯のざくろ石－エジリン - オージャイト片岩中の単斜輝石．島根大学地球資源環境学研究報告，32, 23-31.

眉山地域の三波川変成帯は泥質片岩，塩基性片岩および珪質片岩からなり，少量のざくろ石藍閃石片岩を伴う．点紋帯と無点紋帯にはざくろ石と単斜輝石（ざくろ石－エジリン - オージャイト片岩）を含む珪質片岩が存在する．そのうち点紋帯のざくろ石－エジリン - オージャイト片岩の主要構成鉱物は石英とフェンジャイトであり，その他に少量の角閃石（鉄藍閃石，マグネシオリーベック閃石，リーベック閃石，マグネシオカトホル閃石，ウィンチ閃石，バロア閃石，鉄バロア閃石），ざくろ石，単斜輝石（エジリン - オージャイト，エジリン，オンファス輝石：X_{Jd} 0.08-0.37）と曹長石を含む．赤鉄鉱，チタン鉄鉱，緑泥石，緑れん石，方解石とチタン石が含まれる場合もある．単斜輝石は，曹長石斑状変晶中の包有物（Cpx1）と基質中（Cpx2）の二つの産状がある．単斜輝石の多くは核部においてひすい輝石成分が高く，縁部に低い累帯構造を示す．この累帯構造はピーク変成作用の後に圧力低下を示している．Cpx1 のひすい輝石成分は Cpx2 より高く，これは単斜輝石の組成が曹長石斑状変晶に包有されることによって保存されたことを示す．

Table 1. Representative chemical compositions of clinopyroxenes from the Bizan garnet–aegirine-augite schists.

Sample	KB 13-1																			
Analysis	212	213	234	241	242	246	347	350	352	353	354	355	356	357	358	359	360	361	362	
	Cpx1	Cpx1	Cpx1	Cpx1	Cpx1	Cpx1	Cpx2	Cpx2	Cpx2	Cpx2	Cpx2	Cpx2	Cpx2	Cpx2	Cpx2	Cpx2	Cpx2	Cpx2	Cpx2	
							Rim	←	←	←	←	←	←	←	←	←	←	←	←	
SiO_2	51.94	52.42	52.61	52.72	52.86	52.83	51.94	52.09	52.23	52.01	52.08	52.13	51.87	52.07	52.33	52.17	52.39	52.37	52.70	
TiO_2	0.01	0.08	0.00	0.05	0.06	0.02	0.03	0.03	0.05	0.01	0.03	0.04	0.03	0.01	0.06	0.04	0.06	0.06	0.05	
Al_2O_3	4.22	5.17	4.95	4.19	4.34	4.86	4.29	4.30	4.66	4.30	4.16	4.15	3.88	4.38	4.54	4.29	4.28	4.24	4.28	
FeO*	21.56	17.17	16.01	16.40	16.25	16.15	18.76	20.96	18.17	17.92	18.15	17.96	17.81	17.12	16.55	16.91	17.11	17.03	16.94	
MnO	0.38	0.79	0.74	0.58	0.69	0.68	0.51	0.30	0.57	0.54	0.62	0.48	0.60	0.61	0.65	0.52	0.69	0.69	0.68	
MgO	3.05	5.06	5.05	5.26	5.12	5.06	4.18	3.04	4.60	4.72	4.72	4.82	4.97	5.26	5.37	5.32	5.40	5.41	5.32	
CaO	6.57	9.22	9.41	9.79	9.64	9.37	7.95	5.90	7.83	8.37	8.61	8.59	9.12	9.10	9.27	9.29	9.31	9.37	9.50	
Na_2O	10.08	8.45	8.26	8.15	8.13	8.17	9.33	10.42	9.21	8.81	8.93	8.79	8.56	8.68	8.64	8.70	8.35	8.54	8.34	
Cr_2O_3	0.00	0.02	0.01	0.05	0.01	0.02	0.01	0.01	0.00	0.05	0.00	0.00	0.03	0.03	0.03	0.01	0.00	0.00	0.00	
Total	97.81	98.38	97.04	97.19	97.10	97.16	97.00	97.05	97.32	96.73	97.30	96.96	96.87	97.26	97.44	97.23	97.59	97.71	97.81	
Cations on the basis of 6 oxygens																				
Si	2.06	2.06	2.05	2.06	2.07	2.06	2.06	2.08	2.05	2.06	2.05	2.06	2.05	2.04	2.04	2.05	2.05	2.05	2.05	
Ti	0.00	0.00	0.00	0.00	0.00	0.00	0.00	0.00	0.00	0.00	0.00	0.00	0.00	0.00	0.00	0.00	0.00	0.00	0.00	
Al	0.20	0.20	0.23	0.19	0.20	0.22	0.20	0.20	0.22	0.20	0.19	0.19	0.18	0.20	0.21	0.20	0.20	0.20	0.20	
Fe*	0.72	0.72	0.52	0.54	0.53	0.53	0.62	0.70	0.60	0.59	0.60	0.59	0.59	0.56	0.54	0.56	0.56	0.56	0.55	
Mn	0.01	0.01	0.02	0.02	0.02	0.02	0.02	0.01	0.02	0.02	0.02	0.02	0.02	0.02	0.02	0.02	0.02	0.02	0.02	
Mg	0.18	0.18	0.29	0.31	0.30	0.29	0.25	0.18	0.27	0.28	0.28	0.28	0.29	0.31	0.31	0.31	0.31	0.32	0.31	
Ca	0.28	0.28	0.39	0.41	0.40	0.39	0.34	0.25	0.33	0.35	0.36	0.36	0.39	0.38	0.39	0.39	0.39	0.39	0.40	
Na	0.78	0.78	0.63	0.62	0.62	0.62	0.72	0.81	0.70	0.68	0.68	0.67	0.66	0.66	0.65	0.66	0.63	0.65	0.63	
Cr	0.00	0.00	0.00	0.00	0.00	0.00	0.00	0.00	0.00	0.00	0.00	0.00	0.00	0.00	0.00	0.00	0.00	0.00	0.00	
Total	4.23	4.23	4.15	4.15	4.14	4.13	4.21	4.23	4.19	4.18	4.18	4.17	4.18	4.17	4.16	4.17	4.16	4.19	4.16	

**Total Fe as FeO*

Sample	KB 13-1																			
Analysis	363	364	365	368	369	370	371	372	373	374	378	379	380	381	382	383	384	385	386	
	Cpx2	Cpx2	Cpx2	Cpx2	Cpx2	Cpx2	Cpx2	Cpx2	Cpx2	Cpx2	Cpx2	Cpx2	Cpx2	Cpx2	Cpx2	Cpx2	Cpx2	Cpx2	Cpx2	
	←	←	←	←	←	←	←	Core	Core	→	→	→	→	→	→	→	→	→	→	
SiO_2	52.33	52.44	52.65	52.33	53.16	52.86	52.33	52.87	53.00	51.96	52.11	52.13	52.23	52.21	53.06	52.87	53.23	53.03	53.35	
TiO_2	0.02	0.04	0.07	0.00	0.05	0.03	0.00	0.04	0.03	0.02	0.03	0.02	0.00	0.05	0.06	0.03	0.07	0.04	0.04	
Al_2O_3	4.07	3.92	4.39	3.96	4.26	4.22	4.17	3.70	4.30	4.16	4.11	4.32	4.34	4.16	4.16	4.16	4.16	4.24	4.13	
FeO*	17.04	16.82	17.02	18.42	17.07	17.33	16.95	16.54	17.39	17.00	16.18	16.41	16.13	16.56	16.78	16.63	16.98	17.12	17.07	
MnO	0.69	0.68	0.68	0.58	0.60	0.69	0.60	0.74	0.76	0.84	0.82	0.74	0.77	0.83	0.75	0.80	0.67	0.88	0.78	
MgO	5.40	5.65	5.36	5.12	5.34	5.31	5.26	5.67	5.40	5.67	5.85	5.87	5.76	5.79	6.03	5.87	5.64	5.68	5.60	
CaO	9.43	9.67	9.21	9.08	9.49	9.20	9.27	10.20	9.63	9.79	9.91	9.94	10.07	10.20	10.15	10.10	9.68	9.74	9.60	
Na_2O	8.45	8.16	8.51	8.70	8.65	8.77	8.47	8.14	8.50	8.15	8.22	7.97	8.03	8.05	7.95	8.05	8.36	8.20	8.35	
Cr_2O_3	0.03	0.04	0.01	0.01	0.06	0.00	0.02	0.00	0.01	0.01	0.02	0.01	0.02	0.01	0.00	0.01	0.01	0.02	0.04	
Total	97.46	97.42	97.90	98.20	98.68	98.41	97.07	97.90	99.02	97.60	97.25	97.41	97.35	97.86	98.94	98.52	98.80	98.95	98.96	
Cations on the basis of 6 oxygens																				
Si	2.05	2.05	2.05	2.05	2.05	2.05	2.06	2.06	2.05	2.04	2.04	2.04	2.04	2.04	2.04	2.04	2.05	2.05	2.05	
Ti	0.00	0.00	0.00	0.00	0.00	0.00	0.00	0.00	0.00	0.00	0.00	0.00	0.00	0.00	0.00	0.00	0.00	0.00	0.00	
Al	0.19	0.18	0.20	0.18	0.19	0.19	0.19	0.17	0.20	0.19	0.19	0.20	0.20	0.19	0.19	0.19	0.19	0.19	0.19	
Fe*	0.56	0.55	0.55	0.60	0.55	0.56	0.56	0.54	0.56	0.56	0.53	0.54	0.53	0.54	0.54	0.54	0.55	0.55	0.55	
Mn	0.02	0.02	0.02	0.02	0.02	0.02	0.02	0.02	0.02	0.03	0.03	0.02	0.03	0.03	0.02	0.03	0.02	0.03	0.03	
Mg	0.32	0.33	0.31	0.30	0.31	0.31	0.31	0.33	0.31	0.33	0.34	0.34	0.34	0.34	0.35	0.34	0.32	0.33	0.32	
Ca	0.40	0.41	0.38	0.38	0.39	0.38	0.39	0.43	0.40	0.41	0.42	0.42	0.42	0.43	0.42	0.42	0.40	0.40	0.40	
Na	0.64	0.62	0.64	0.66	0.65	0.66	0.65	0.61	0.64	0.62	0.62	0.60	0.61	0.61	0.59	0.60	0.63	0.61	0.62	
Cr	0.00	0.00	0.00	0.00	0.00	0.00	0.00	0.00	0.00	0.00	0.00	0.00	0.00	0.00	0.00	0.00	0.00	0.00	0.00	
Total	4.18	4.16	4.15	4.19	4.16	4.17	4.18	4.16	4.18	4.18	4.17	4.16	4.17	4.18	4.15	4.16	4.16	4.16	4.16	

**Total Fe as FeO*

Sample	KB 13-1																			
Analysis	387	388	389	390	391	495	496	497	498	499	500	501	502	503	504	505	506	507	627	
	Cpx2	Cpx2	Cpx2	Cpx2	Cpx2	Cpx1	Cpx1	Cpx1	Cpx1	Cpx1	Cpx1	Cpx1	Cpx1	Cpx1	Cpx1	Cpx1	Cpx1	Cpx1	Cpx1	
	→	→	→	→	Rim	Rim	←	←	←	←	←	Core	→	→	→	→	→	Rim		
SiO_2	53.29	53.22	53.36	53.09	53.47	52.75	52.55	53.02	53.64	53.78	53.67	54.15	53.92	53.98	53.62	52.30	52.52	52.69	52.75	
TiO_2	0.06	0.03	0.02	0.04	0.04	0.03	0.00	0.04	0.05	0.00	0.05	0.02	0.03	0.01	0.04	0.02	0.03	0.04	0.04	
Al_2O_3	4.03	4.10	3.91	3.79	4.02	4.79	4.81	4.72	7.82	8.24	8.53	8.31	8.15	8.25	8.04	4.85	4.67	4.70	4.85	
FeO*	17.46	17.44	18.16	18.76	18.63	16.86	16.59	16.63	15.98	15.33	15.78	15.66	15.85	15.93	15.64	16.72	16.65	17.07	16.08	
MnO	0.77	0.60	0.58	0.57	0.54	0.62	0.68	0.72	0.46	0.42	0.45	0.40	0.42	0.57	0.46	0.61	0.65	0.55	0.64	
MgO	5.69	5.46	5.36	4.83	4.83	5.32	5.50	5.62	3.60	3.40	3.33	3.48	3.56	3.41	3.63	5.25	5.55	4.92	5.49	
CaO	9.78	9.58	9.52	8.75	8.80	9.17	9.32	9.64	5.95	5.52	5.33	5.71	5.66	5.67	5.98	9.01	9.60	9.04	9.65	
Na_2O	8.17	8.19	8.48	8.94	9.09	8.36	8.26	8.30	10.41	10.68	10.86	10.77	10.66	10.75	10.35	8.49	8.32	8.49	8.05	
Cr_2O_3	0.00	0.00	0.04	0.02	0.01	0.00	0.00	0.03	0.00	0.01	0.00	0.02	0.02	0.01	0.00	0.01	0.00	0.00	0.00	
Total	99.25	98.62	99.43	98.79	99.43	97.90	97.71	98.72	97.91	97.38	98.00	98.52	98.27	98.58	97.76	97.26	97.99	97.50	97.55	
Cations on the basis of 6 oxygens																				
Si	2.05	2.06	2.05	2.06	2.06	2.05	2.04	2.04	2.05	2.06	2.05	2.05	2.05	2.05	2.05	2.04	2.04	2.06	2.05	
Ti	0.00	0.00	0.00	0.00	0.00	0.00	0.00	0.00	0.00	0.00	0.00	0.00	0.00	0.00	0.00	0.00	0.00	0.00	0.00	
Al	0.18	0.19	0.18	0.17	0.18	0.22	0.22	0.21	0.35	0.37	0.38	0.37	0.37	0.37	0.36	0.22	0.21	0.22	0.22	
Fe*	0.56	0.56	0.58	0.61	0.60	0.55	0.54	0.54	0.51	0.49	0.50	0.50	0.50	0.51	0.50	0.55	0.54	0.56	0.52	
Mn	0.03	0.02	0.02	0.02	0.02	0.02	0.02	0.02	0.01	0.01	0.01	0.01	0.01	0.02	0.01	0.02	0.02	0.02	0.02	
Mg	0.33	0.31	0.31	0.28	0.28	0.31	0.32	0.32	0.21	0.19	0.19	0.20	0.20	0.19	0.21	0.31	0.32	0.29	0.32	
Ca	0.40	0.40	0.39	0.36	0.36	0.38	0.39	0.40	0.24	0.23	0.22	0.23	0.23	0.23	0.25	0.38	0.40	0.38	0.40	
Na	0.61	0.61	0.63	0.67	0.68	0.63	0.62	0.62	0.77	0.79	0.80	0.79	0.79	0.79	0.77	0.64	0.63	0.64	0.61	
Cr	0.00	0.00	0.00	0.00	0.00	0.00	0.00	0.00	0.00	0.00	0.00	0.00	0.00	0.00	0.00	0.00	0.00	0.00	0.00	
Total	4.16	4.15	4.16	4.17	4.18	4.16	4.15	4.15	4.14	4.14	4.15	4.15	4.15	4.16	4.15	4.16	4.16	4.17	4.14	

**Total Fe as FeO*

Table 1. (continued)

Sample	KB 14-3																			
Analysis	125	126	127	128	129	130	131	132	133	134	135	136	137	142	143	144	145	146	147	
	Cpx2	Cpx2	Cpx2	Cpx2	Cpx2	Cpx2	Cpx2	Cpx2	Cpx2	Cpx2	Cpx2	Cpx2	Cpx2	Cpx2	Cpx2	Cpx2	Cpx2	Cpx2	Cpx2	
	Rim	←	←	←	←	←	←	←	←	←	←	←	Core	→	→	→	→	→	→	
SiO_2	53.96	53.61	53.26	53.47	53.22	53.37	53.00	53.41	53.72	54.05	54.22	53.70	53.76	53.32	53.26	53.40	52.93	53.16	53.24	
TiO_2	0.06	0.05	0.01	0.05	0.01	0.04	0.01	0.06	0.02	0.06	0.06	0.05	0.05	0.03	0.02	0.04	0.02	0.01	0.06	
Al_2O_3	4.18	4.00	3.90	3.71	4.05	4.12	4.78	5.44	5.65	5.71	5.69	5.41	4.57	4.01	4.09	4.29	4.39	4.17	3.86	
FeO*	19.30	18.51	18.46	18.50	17.84	17.66	17.85	17.18	17.19	16.98	17.23	16.78	17.05	16.77	17.67	17.78	16.94	18.10	18.65	
MnO	0.56	0.53	0.66	0.57	0.59	0.75	0.73	0.67	0.75	0.77	0.62	0.78	0.65	0.69	0.73	0.66	0.74	0.68	0.61	
MgO	4.43	4.55	4.87	5.12	5.34	5.80	5.15	4.87	4.69	4.78	4.68	4.97	5.58	5.88	5.55	5.10	5.50	5.24	4.68	
CaO	8.08	8.32	8.78	9.27	9.46	9.94	8.54	7.75	7.86	7.84	7.54	8.20	9.15	10.29	9.52	9.06	9.86	9.37	8.99	
Na_2O	9.34	9.30	8.80	8.70	8.57	8.28	9.15	9.53	9.56	9.39	9.80	9.19	8.47	8.11	8.63	8.82	8.42	8.53	8.97	
Cr_2O_3	0.01	0.03	0.01	0.03	0.02	0.02	0.02	0.00	0.00	0.00	0.00	0.00	0.00	0.00	0.00	0.00	0.02	0.00	0.00	
Total	99.92	98.87	98.76	99.42	99.10	99.98	99.23	98.91	99.44	99.58	99.84	99.08	99.28	99.10	99.47	99.15	98.82	99.26	99.06	
Cations on ti .																				
Si	2.07	2.07	2.07	2.06	2.05	2.04	2.04	2.05	2.05	2.06	2.06	2.05	2.06	2.05	2.05	2.06	2.04	2.05	2.06	
Ti	0.00	0.00	0.00	0.00	0.00	0.00	0.00	0.00	0.00	0.00	0.00	0.00	0.00	0.00	0.00	0.00	0.00	0.00	0.00	
Al	0.19	0.18	0.18	0.17	0.18	0.19	0.22	0.25	0.25	0.26	0.25	0.24	0.21	0.18	0.19	0.19	0.20	0.19	0.18	
Fe*	0.62	0.60	0.60	0.60	0.58	0.56	0.58	0.55	0.55	0.54	0.55	0.54	0.55	0.54	0.57	0.57	0.55	0.58	0.60	
Mn	0.02	0.02	0.02	0.02	0.02	0.02	0.02	0.02	0.02	0.02	0.02	0.03	0.02	0.02	0.02	0.02	0.02	0.02	0.02	
Mg	0.25	0.26	0.28	0.29	0.31	0.33	0.30	0.28	0.27	0.27	0.26	0.28	0.32	0.34	0.32	0.29	0.32	0.30	0.27	
Ca	0.33	0.34	0.36	0.38	0.39	0.41	0.35	0.32	0.32	0.32	0.31	0.34	0.38	0.42	0.39	0.37	0.41	0.39	0.37	
Na	0.69	0.70	0.66	0.65	0.64	0.61	0.68	0.71	0.71	0.69	0.72	0.68	0.63	0.60	0.64	0.66	0.63	0.64	0.67	
Cr	0.00	0.00	0.00	0.00	0.00	0.00	0.00	0.00	0.00	0.00	0.00	0.00	0.00	0.00	0.00	0.00	0.00	0.00	0.00	
Total	4.17	4.17	4.17	4.17	4.17	4.16	4.19	4.18	4.17	4.16	4.17	4.16	4.17	4.15	4.18	4.16	4.17	4.17	4.17	

**Total Fe as FeO*

Sample	KB 14-3																			
Analysis	148	149	150	151	152	204	205	206	207	208	209	218	219	220	221	222	223	224	225	
	Cpx2	Cpx2	Cpx2	Cpx2	Cpx2	Cpx1	Cpx1	Cpx1	Cpx1	Cpx1	Cpx1	Cpx1	Cpx1	Cpx1	Cpx1	Cpx1	Cpx1	Cpx1	Cpx1	
	→	→	→	→	Rim	Rim	←	Core	→	→	Rim	Rim	←	←	Core	→	→	Rim		
SiO_2	53.35	53.49	53.33	53.16	52.65	53.18	53.33	53.61	52.99	53.37	53.46	53.55	53.41	53.03	52.66	52.99	53.16	53.15	51.95	
TiO_2	0.00	0.06	0.05	0.05	0.00	0.05	0.04	0.04	0.03	0.04	0.02	0.01	0.08	0.03	0.06	0.02	0.03	0.01	0.06	
Al_2O_3	3.74	3.81	3.79	3.23	2.70	5.78	6.02	6.69	5.78	5.38	5.05	5.98	5.77	5.26	4.12	4.42	4.78	4.99	3.10	
FeO*	19.39	19.37	19.41	19.52	21.98	16.40	16.36	15.81	15.79	16.21	16.22	16.52	16.17	16.35	16.15	16.70	16.30	16.09	23.41	
MnO	0.51	0.46	0.56	0.57	0.49	0.70	0.66	0.61	0.78	0.78	0.71	0.66	0.70	0.74	0.75	0.79	0.81	0.88	0.33	
MgO	4.44	4.45	4.27	4.88	3.32	4.91	4.72	4.29	5.09	5.31	5.32	4.62	4.94	5.18	6.02	5.65	5.49	5.41	2.09	
CaO	8.63	8.44	8.28	9.17	8.95	8.20	7.70	7.25	8.81	8.99	9.07	7.79	8.43	8.83	10.48	9.88	9.56	9.36	6.27	
Na_2O	9.29	9.28	9.48	8.93	9.07	9.04	9.45	9.81	8.78	8.85	8.68	9.35	9.17	8.71	7.85	8.13	8.38	8.63	10.34	
Cr_2O_3	0.00	0.03	0.00	0.00	0.00	0.00	0.04	0.02	0.01	0.00	0.01	0.00	0.00	0.07	0.05	0.08	0.08	0.04	0.00	
Total	99.34	99.39	99.17	99.51	99.16	98.26	98.32	98.13	98.06	98.93	98.54	98.48	98.67	98.20	98.14	98.66	98.59	98.56	97.55	
Cations on the basis of 6 oxygens																				
Si	2.07	2.07	2.07	2.06	2.08	2.05	2.05	2.05	2.04	2.04	2.05	2.05	2.05	2.05	2.04	2.05	2.05	2.05	2.09	
Ti	0.00	0.00	0.00	0.00	0.00	0.00	0.00	0.00	0.00	0.00	0.00	0.00	0.00	0.00	0.00	0.00	0.00	0.00	0.00	
Al	0.17	0.17	0.17	0.15	0.13	0.26	0.27	0.30	0.26	0.24	0.23	0.27	0.26	0.24	0.19	0.20	0.22	0.23	0.15	
Fe*	0.63	0.63	0.63	0.63	0.72	0.53	0.53	0.51	0.51	0.52	0.52	0.53	0.52	0.53	0.52	0.54	0.53	0.52	0.79	
Mn	0.02	0.02	0.02	0.02	0.02	0.02	0.02	0.02	0.03	0.03	0.02	0.02	0.02	0.02	0.02	0.03	0.03	0.03	0.01	
Mg	0.26	0.26	0.25	0.28	0.20	0.28	0.27	0.25	0.29	0.30	0.30	0.26	0.28	0.30	0.35	0.33	0.32	0.31	0.13	
Ca	0.36	0.35	0.34	0.38	0.38	0.34	0.32	0.30	0.36	0.37	0.37	0.32	0.35	0.37	0.44	0.41	0.39	0.39	0.27	
Na	0.70	0.70	0.71	0.67	0.69	0.67	0.70	0.73	0.66	0.66	0.65	0.70	0.68	0.65	0.59	0.61	0.63	0.64	0.81	
Cr	0.00	0.00	0.00	0.00	0.00	0.00	0.00	0.00	0.00	0.00	0.00	0.00	0.00	0.00	0.00	0.00	0.00	0.00	0.00	
Total	4.21	4.20	4.19	4.19	4.22	4.15	4.16	4.16	4.15	4.16	4.14	4.13	4.16	4.16	4.15	4.17	4.17	4.17	4.25	

**Total Fe as FeO*

Sample	KB 05																			
Analysis	147	148	149	150	151	152	153	154	155	156	157	158	159	160	161	162	163	164	165	
	Cpx2	Cpx2	Cpx2	Cpx2	Cpx2	Cpx2	Cpx2	Cpx2	Cpx2	Cpx2	Cpx2	Cpx2	Cpx2	Cpx2	Cpx2	Cpx2	Cpx2	Cpx2	Cpx2	
	Rim	←	←	←	←	Core		Core	→	→	→	→	→	→	Rim					
SiO_2	52.44	52.63	52.67	52.86	52.63	52.65	53.09	53.66	53.33	52.94	53.17	53.11	53.29	53.27	53.10	53.14	53.14	52.84	54.22	
TiO_2	0.00	0.03	0.00	0.00	0.00	0.00	0.03	0.00	0.00	0.00	0.00	0.00	0.02	0.00	0.02	0.00	0.01	0.02	0.06	
Al_2O_3	2.37	2.82	4.49	4.36	3.93	4.12	4.77	3.94	3.09	2.96	3.28	4.42	4.14	3.71	2.76	3.24	4.51	4.20	5.24	
FeO*	18.06	18.34	16.85	17.20	17.30	17.08	16.37	15.84	16.58	16.66	17.19	16.15	16.20	17.67	19.16	17.63	16.27	17.33	15.11	
MnO	0.70	0.52	0.48	0.46	0.35	0.41	0.39	0.45	0.28	0.42	0.32	0.52	0.43	0.41	0.44	0.55	0.44	0.25	0.45	
MgO	5.65	5.28	5.39	5.47	5.29	5.17	5.45	6.40	6.48	6.70	6.44	5.96	5.78	5.11	5.03	5.96	5.74	5.02	5.97	
CaO	10.33	9.32	9.67	9.82	9.96	9.83	9.42	11.12	12.09	12.46	11.84	10.25	10.00	9.36	9.68	10.43	9.93	9.62	9.41	
Na_2O	8.25	8.55	8.46	8.31	8.30	8.30	8.61	7.81	7.01	6.72	7.14	8.13	8.38	8.67	8.53	8.09	8.23	8.28	9.02	
Cr_2O_3	0.00	0.00	0.00	0.00	0.00	0.00	0.02	0.00	0.00	0.00	0.00	0.00	0.04	0.02	0.00	0.02	0.00	0.00	0.00	
Total	97.80	97.49	98.01	98.48	97.76	97.56	98.15	99.22	98.86	98.86	99.38	98.54	98.28	98.22	98.72	99.06	98.27	97.56	99.48	
Cations on the basis of 6 oxygens																				
Si	2.07	2.07	2.05	2.05	2.06	2.06	2.05	2.05	2.06	2.05	2.04	2.05	2.06	2.07	2.07	2.05	2.05	2.06	2.05	
Ti	0.00	0.00	0.00	0.00	0.00	0.00	0.00	0.00	0.00	0.00	0.00	0.00	0.00	0.00	0.00	0.00	0.00	0.00	0.00	
Al	0.11	0.13	0.21	0.20	0.18	0.19	0.22	0.18	0.14	0.13	0.15	0.20	0.19	0.17	0.13	0.15	0.21	0.19	0.23	
Fe*	0.60	0.60	0.55	0.56	0.57	0.56	0.53	0.51	0.53	0.54	0.55	0.52	0.52	0.57	0.63	0.57	0.53	0.57	0.48	
Mn	0.02	0.02	0.02	0.02	0.01	0.01	0.01	0.01	0.01	0.01	0.01	0.02	0.01	0.01	0.01	0.02	0.01	0.01	0.01	
Mg	0.33	0.31	0.31	0.32	0.31	0.30	0.31	0.36	0.37	0.39	0.37	0.34	0.33	0.30	0.29	0.34	0.33	0.29	0.34	
Ca	0.44	0.39	0.40	0.41	0.42	0.41	0.39	0.46	0.50	0.52	0.49	0.42	0.41	0.39	0.41	0.43	0.41	0.40	0.38	
Na	0.63	0.65	0.64	0.62	0.63	0.63	0.65	0.58	0.52	0.50	0.53	0.61	0.63	0.65	0.65	0.61	0.62	0.63	0.66	
Cr	0.00	0.00	0.00	0.00	0.00	0.00	0.00	0.00	0.00	0.00	0.00	0.00	0.00	0.00	0.00	0.00	0.00	0.00	0.00	
Total	4.20	4.17	4.18	4.18	4.18	4.16	4.16	4.15	4.13	4.14	4.14	4.16	4.15	4.16	4.17	4.17	4.16	4.15	4.15	

**Total Fe as FeO*